Additional Topics: Techniques of Inertial Navigation

Dr John K Fawcett

2005-03-14

Contents

List of Figures

List of Tables

Chapter 1

Techniques of Inertial Navigation

Inertial Navigation has scientific basis in Newton's laws of motion. Those skilled in the art employ instruments designed to detect and quantise relative velocities or accelerations of rigid bodies through vector fields. Position fixes are obtained from sensor measurements by single or double integration with respect to time; the constant of integration depends on the origin of motion[32]. Throughout the last 120 years physical scientists have studied Inertial Navigation through the magnetic and gravitational fields caused by the Earth and so developed a comprehensive understanding of the theory and practice of locating objects, and associated sources of error.

1.1 Gyroscopes

French physicist Jean Foucault first applied the term *gyroscope* to a rotating mass supported by a gimbal ring in 1853. Figure 1.1(a) illustrates a single-degree-of-freedom (SDF) gyro, also known as a *captive* gyro because the spin axis is forced to rotate with the gyro case[8]. An electrical signal applied to the Torque Generator (TG) input causes a torque on the angular momentum and is used to apply corrections.

(a) Single-Degree-of-Freedom Gyro   (b) Two-Degrees-of-Freedom Gyro
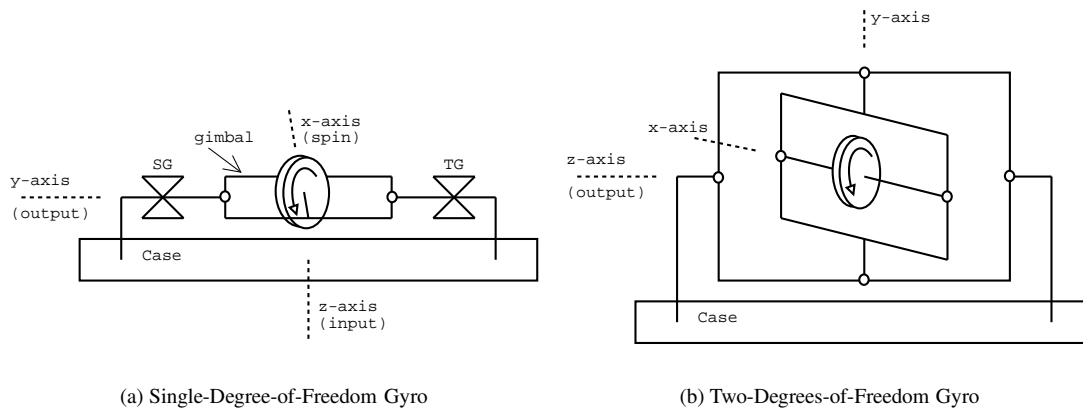
Figure 1.1: Rotating Mass Gyroscopes

In unmanned aircraft and ballistic missiles it injects course data which, though a closed feedback loop to steering servos, allows the device to follow a predefined route[42]. Angular rotation of the case in a field under torque T_i about the input axis causes the gyro to precess about the output axis with rate Ω:

$$\mathbf{L} = I\omega_{\mathbf{g}} \tag{1.1}$$

$$\Omega = \frac{T_i}{|\mathbf{L}|} \tag{1.2}$$

where $\mathbf{L}$ is the angular momentum vector of the gyro parallel to the spin axis, I is the moment of inertia of the gyro about the spin axis, and ω_g is the angular velocity vector of the gyro about the spin axis[12]. Voltages proportional to the angular deviation of the gimbal with respect to the case are produced by moving coil pickoffs on the gimbal frame, amplified and fed to the Signal Generator (SG) output. A *rate* gyro is a captive gyro with an elastic restraint preventing precession and is sensitive to rate of angular motion of the spin axis through the field. Such motion causes the gyro to seek a gyroscopic-restraint torque balance, manifested as a deflection in the angle of the gimbal with respect to the case which will nullify when the angular motion ceases. Under these circumstances the SG output is proportional to the input rate.

Two-degrees-of-freedom (TDF) or *free* gyros, shown in Figure 1.1(b), are also known as *amount* or *displacement* gyros when used to measure angular displacements[39]. Damping the precessional motion gives a rate-integrating gyro whose output is proportional to the time integral of the input. Three-degrees-of-freedom gyros are also used but have disproportionate bulk due to the inclusion of a fourth ("redundant") gimbal ring required to prevent gimbal lock (a mutual alignment of two gimbal axes caused by a $90°$ rotation resulting in the loss of one degree of freedom)[40].

1.1.1 Floated Gyros

No TDF gyro perfectly maintains the original reference orientation and no SDF gyro accurately measures angular deflections indefinitely. Accruing errors known as *drift* gradually reduce accuracy and in lower specification gyros are dominated by ball bearing friction at the gimbal pivots. Drift rates of $100°$/hr are acceptable for many applications but Inertial Navigation necessitates advanced techniques and "friction-less" bearings. Floated gyros distinguish two duties of the pivots: support and axis definition[6]. Drift rates better than $0.1°$/hr can be achieved. The idea of supporting the mass of the gyro in a viscous fluid of density equal to the average density of the gyro and gimbal frame—neutral buoyancy—is attributed to Schuler and Anschutz (1911) although it was after World War II when Dr CS Draper commercialised his work at Massachusetts Institute of Technology on the HIG5 (hermetic integrating gyro with angular momentum 10^5 c.g.s. units) through the Honeywell Regulator Company. Pivot-and-jewel constructions are used to ensure axis alignment and the construction is hermetically sealed. A heater maintains the viscous fluid at operating temperature and density, and bellows absorb excess pressure caused by thermal expansion.

Fluid-floated gyros are restrained because construction constraints permit only very small angular deviations: small angle approximations apply and serve to reduce computational complexity; cross coupling of the output axes in TDF gyros also contributes negligible error. Other floatation techniques are still in use[3]: flexures, pressurised air jets, highly stable magnetic fields achieved through cryogenics provide passive support, and electrically supported gyros (ESG)—true displacement gyros—use optical sensors to read a coded pattern on the surface of a suspended sphere (the gyro) free to rotate (without power after

spin-up) in a high vacuum; the engineering challenge is often achieving the degree of support stiffness required for high precision.

1.1.2   Vibrating Structure Gyros (VSG)

A VSG transducer consists of a piezoceramic cylindrical cup furnished with alternating drive and sense electrodes on the outer sides. The rim is made to resonate between two oval states such that four nodes on the rim achieve minimal oscillation amplitude. The transducer is mechanically supported only by a stem constructed to preclude interference with the resonant motion. Momentum associated with the vibration gyroscopically maintains the orientation of the mass of the cylinder. Rotation of the cylinder about its principal (stem) axis causes the four points to rotate into the driven vibration and the sense electrodes to emit a signal proportional to the angular rotation. Compensation tolerates moderate non-uniformity of the piezoceramic material and error depends on the rate of decay of oscillations and any active response in the controlling electronics. Decay rate represents the bandwidth of the transducer and is dominated by the Q-factor (quality) of the material and the natural frequency of the arrangement.

Watson describes in his patent report[50] numerous error reducing enhancements to a basic design which use Lead Zirconium Titanate (PZT) ceramics to relax manufacturing tolerances, novel drive electrode shapes to increase efficiency and suppress unwanted modes of oscillation, narrow sense electrodes to minimise the effects of thermal imbalances, and uniform polarisation techniques to negate thermal hysteresis caused by accumulating charges within the ceramic. Keyed cup shapes improve reliability of fly-lead contacts and a grounding contact fed through the stem eliminates interference to the vibratory motion.

BAe Systems (Plymouth, England) were awarded a Millennium Award on 2nd November 1998 for a micromachined silicon ring gyroscope or SiVSG[1]. Three SiVSG devices are used in the wings of Airbus A340-500 family aircraft and in multifunction naval radars.

Table 1.1: Errors affecting Gyro-Stabilised Platforms

Errors affecting Gyro-Stabilised Platforms[39, 9, 41]	
Error	*Description and Treatment*
Non-g-sensitive	
Flex lead drag and magnetic reaction torque	Constant-with-time drift rate observed in restraint gyros. The magnitude of each can be measured and compensated although precise measurement is hindered by noise and long time averages are required for high precision. Calibration is usually performed to 1σ of the random component.
Storage temperature drift	The calibrations above are temperature-sensitive and can shift significantly with temperature when the gyro falls below operating temperature. Manufacturers typically quote bounds on the shift over the range of storage temperatures permitted by the device. Where the shift is not acceptable arrangements are made to maintain power during shipping, or to repeat the calibration after installation.
continued on next page	

Error	*Description and Treatment*
	continued from previous page
Magnetic fields	A constant field strength causes constant-with-time drift. The amplitude varies sinusoidally with the angle of the gyro relative to the field. The gyro case is typically designed to prevent external field interaction.
Computer processing and control	Floating-point errors in control, calibration, and correction software can introduce errors into the system. Timing errors in issuing commands to the gyroscope (via the TG input) yield position errors proportional to the tardiness and velocity.
g-sensitive	
Gimbal mass imbalance	This gives rise to a drift rate under linear acceleration which varies sinusoidally as the gyro is rotated about its output axis in the acceleration field. Factory calibration is possible but storage temperature effects as above limit the effectiveness of such approaches.
External temperature	Changes in ambient temperature in the block cavity where the gyro is mounted can lead to drift, as can local thermal variations caused by draughts. Draught correction coefficients vary proportionally to an applied acceleration and the magnitude of the draught velocity, and sinusoidally with the orientation of the gyro with respect to the draught velocity.
Alignment errors	Imprecise initial alignment of a gyrostabilised platform or accelerometer triad leads to significant error. It is essential to accurately characterise the initial configuration.
Gyro misalignment	In Schuler-Tuned configurations, misaligned stabilisation gyros contribute to platform error, and thus net error.
Anisoelastic drift	Unequal elasticity along the spin and input axes gives rise to steady-state drift when linear or vibratory accelerations act on both axes simultaneously. The drift rate varies with applied linear acceleration or vibration and varies sinusoidally as the gyro is rotated about the output axis in the acceleration environment. The drift caused by rotation has a $sin(2\theta)$ characteristic which is exploited by a Tumbling Test to separate out the anisoelastic coefficient. The anisoelastic coefficient is zero when perturbations do not act on both axes simultaneously so it is common to align the axes with gravity and any engine thrust vector. Vibrations often average to zero and are usually assumed to do so with spherical randomness of direction (since the direction of vibration is unknown during design). Upper bounds on the errors due to vibration, including anisoinertial, cylindrical and coning effects, can be found and are sometimes quoted by manufacturers.
	continued on next page

	continued from previous page
Error	*Description and Treatment*
Non-uniform g field	The Earth's gravitation field deviates from spherical uniformity. Inaccurate electronic modelling yields negligible error provided maximum displacement is small. Otherwise precision will vary with position.
Random	"Random" is the collective term describing those effects left uncalibrated, and residual errors after calibration. Errors in this class are measured statistically in order to determine the standard deviation and thus the degree of calibration which will pay dividends in reducing error.
Local-Vertical Configurations	
Earth spin	It is common practice to correct for the rotation of the earth beneath an airborne vessel.
Local velocity	North and East gyros are often corrected for the vehicle's movement, otherwise long trajectories lead to significant position error at the destination.

1.2 Accelerometers

An odometer and gyroscope can be used for crude navigation and such arrangements underlie several dead reckoning augmentations to GPS sets. Gyros are commonly used to drive servos to stabilise a platform in an inertial frame. Highly precise velocity and distance measurements can be obtained by time-integrating the outputs of three mutually perpendicular accelerometers secured to such a platform[10]. Table 1.1 enumerates the sources of error in gyro-stabilisation[39, 9] and the techniques used to minimise, eliminate, or compensate for their effects[41].

1.2.1 Pendulous Accelerometers

Floated pendulums, flexure supported pendulums and pendulous gyro integrating accelerometers (PGIA or PIGA)—collectively pendulous accelerometers—were first used for this purpose. The addition of a motor providing resistive torque proportional to the input acceleration introduces a second integration making the output voltage proportional to the displacement from the start of motion. Table 1.2 summarises errors in pendulous accelerometers[10].

1.2.2 Non-Pendulous Accelerometers

Non-pendulous devices include pneumatic, vibrating string, and angular accelerometers. Figure 1.2 illustrates the construction of a Vibrating String Accelerometer (VSA). The natural or resonant frequency, ω_{res},
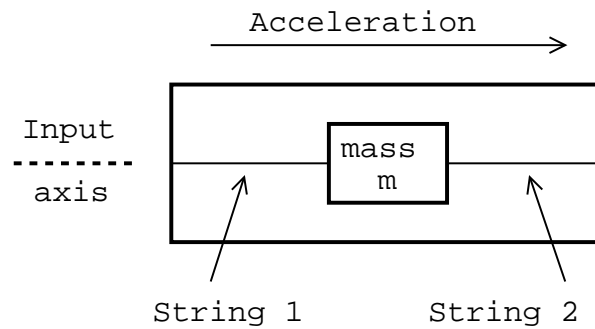
Figure 1.2: Construction of a Vibrating String Accelerometer

of small amplitude, transverse vibrations in a taut string is related to the tension, T, in the string by

$$\omega_{res} = \frac{\pi}{L} \left(\frac{T}{\mu} \right)^{1/2}$$

(1.3)

where μ is the mass per unit length of the string of length L[11]. Linear acceleration along the input axis causes reaction forces in the strings to accelerate the central mass, changing their tensions and thus natural frequencies of oscillation according to Equation 1.3. Sensors detect the changes in natural frequency and a voltage dependant on the input acceleration is available. Correction factors for the change in total tension must be applied and a device non-linearity profile handles other significant sources of error. However, the need to overcome static friction of the mass in its guide renders VSAs unable to respond to small accelerations and causes null uncertainty from which position errors can rapidly accrue. Integrating non-pendulous accelerometers produce output proportional to the velocity of the device[38] and, due to the internal integration, certain (random) dynamic errors average to zero and thus do not contribute noise to the output.

Table 1.2: Errors affecting Pendulous Accelerometers

Errors affecting Pendulous Accelerometers[10]	
Error	*Description and Treatment*
Null uncertainty	Static friction at the pivot causes non-repeatability of the zero position. The error is a constant offset in acceleration, a steadily increasing error in velocity, and a rapidly growing error in position. Lubricants are applied to the bearings of lower specification gyros to combat static friction and higher precision instruments use pivot-and-jewel or frictionless bearings.
Non-pendulous torque shift	Temperature reductions below the operating temperature after calibration cause a constant shift in calibration parameters with deeper chills leading to larger offsets. Manufacturers typically quote bounds on the shift over the range of storage temperatures permitted by the device. Where the shift is not acceptable arrangements are made to maintain power during shipping, or to repeat the calibration after installation.
continued on next page	

Error	*Description and Treatment*
	continued from previous page
Scale factors	Any non-linearity of gimbal pendulosity with respect to that torque–current relationship (which is not modelled and compensated) leads to error.
Cross coupling	Marginal imperfections in axis orthogonality cause significant errors under strong accelerations and retardations, and accumulate in significance over time. Axis alignment is often adjusted in factory calibration of accelerometer triads.
Vibropendulous error	Simultaneous vibration along input and pendulous axes gives rise to a vibropendulous effect which can be characterised for sinusoidal vibrations (and compensations applied). Vibrations are usually unpredictable, however, and are minimised by geometric orientations where a component of gravity, g, acts along all three accelerometer axes of a gyrostabilised platform triad accelerometer.

1.3 Errors in Inertial Navigation

Sources of imprecision are well understood (Tables 1.1, 1.2) and instruments assembled to various tolerances. Position errors at the destination, present after compensation and calibration, are deviations from the intended location and are often resolved into components along course (range), ϵ_{ac}, and cross course, ϵ_{cc}. The root-sum-square error, ϵ_{rss}, defined as

$$\epsilon_{rss} = \sqrt{\epsilon_{ac}^2 + \epsilon_{cc}^2} \qquad (1.4)$$

is used as a total error metric. Course position errors during thrust and ballistic phases of unmanned travel—differences between actual positions and those detailed in a predetermined flight plan—are expressed in terms of time. For example, any offset at the moment a trajectory correction manoeuvre (TCM) is applied is described by the vessel being early or late of its flight plan. Course velocity errors are expressed in absolute terms but are quoted only at disparate, identifiable points. It is common avionic practice to state the velocity (and position) course error at the engine cut-off (ECO) point.

Chapter 2

Nautical Navigation Aids

2.1 Celestial Navigation

Navigation at sea is an enigmatic engagement with no assistance from the coastal landmarks used by littoral helmsmen to determine bearings using a pelorus. Positioning resolution of 1 or 2 miles was regularly achieved by trained seamen in clear weather by celestial navigation[20]. Precise inclinations of celestial bodies can be measured using a sextant with the sea as a natural horizon and a position fix obtained with reference to an almanac by intersecting circular loci on appropriate charts using spherical geometry[51]. Stars were selected so as to maximise the acute intersection angles when cloud cover allowed and thus minimise geometric error. Bubble-level artificial horizons act as reference in aircraft but the ultimate horizontal precisions of fixes fall between 10 and 20 miles. Aircraft climb "above the weather" to increase accuracy and obtain a fix despite overcast conditions on the surface. Fully automated electronic celestial navaids are capable of deriving geocentric longitude and latitude using photovoltaic, photoconductive or photoemissive components to survey the night sky[17].

Twentieth century advances in radio engineering afforded higher precision, hyperbolic positioning systems. Synchronized *master* and *slave* stations transmit identical signals from physically disparate, coastal locations. Navigators require only radio receiving equipment: an arbitrary number of users can be supported simultaneously and they need not risk revealing their locations to others by transmitting. Receiver operators place their location on a hyperbolic curve by monitoring the time difference of arrival through phase-difference observations of the coherent transmissions from two stations (Figure 2.1); by repeating this for two or more pairs of stations a position fix can be established[43].

2.2 Gee

Gee (Outfit QH) was a British implementation originally proposed by RJ Dippy which operated from March 1942 in the European Theatre of World War II. Pulsed codes (full-range amplitude-modulated carriers) were transmitted at 20–85 MHz by stations radiating 300 kW. Availability ranged from 150 statute miles at surface altitude to 450 miles at 30 000 ft[20]. Pulse durations were 6 μs and the phase differences of
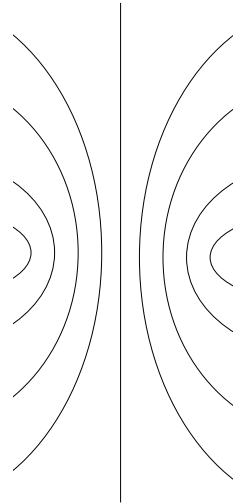
Figure 2.1: Fixing using a hyperbolic radio navigation system. The hyperbolae are contours of constant phase difference.

Table 2.1: Drawbacks of RJ Dippy's Gee Hyperbolic Radio Navaid (1942)

Limited range	The 20–85 MHz carrier frequency gave good range only at high altitude rendering Gee largely unsuitable for naval operation.
Base line length	The pulse code recurrence rates adopted by Gee stations limited the base line length and thus geometric advantage.
Spectrum inefficiency	Only one set of co-operating master/slave stations could be operated per 0.5 MHz of spectrum, a large bandwidth.
Practical difficulties	Differing path loss between the receiver and the stations in use caused pulse amplitudes to vary on the oscilloscope trace. Only experienced operators possessed the skill and judgement necessary to obtain an accurate fix. This also made fix automation impractical with the technology of the day.

pulse trains characteristic of coherent stations were measured manually using a fast-scan cathode ray tube oscilloscope as a comparator. An experienced operator was able to measure time differences of arrival to an accuracy of 0.6 μs. Fix errors are proportional to linear timing errors and inversely proportional to the sine of the angle between hyperbolae at intersection points. The latter decreases approximately inversely with range so fix errors are proportional to the square of distance from transmitters. At close range the user position error was 200 yards and approximately 1 mile at 450 miles range. Positions, and speeds obtained by finite differences, were true ground positions and speeds—a particular advantage to aircraft pilots for homing and course tracking. Gee offered *instantaneous fixing* allowing the user to determine the parameters of two or more hyperbolae simultaneously (the process of doing so took some 90 seconds) which gave significantly improved performance compared to identifying hyperbolae in succession, especially to rapidly moving objects. Gee was jammable and suffered a number of technical drawbacks (Table 2.1), and was eventually phased out.
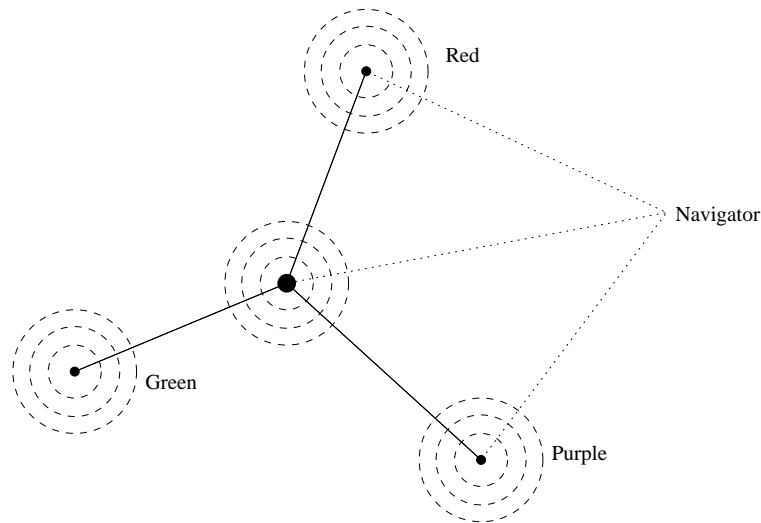
Figure 2.2: A typical Decca installation (this from north Germany): central master with radial slaves

2.3   Decca Navigator

Conceived in 1939 by American WJ O'Brien and officially designated "Outfit QM" the Decca Navigator was a low frequency, continuous wave hyperbolic radio navaid service initially run by the British Admiralty in areas close to British shores as an alternative to the readily jammable Gee system[15]. In 1999 the British General Lighthouse Authority (BGLA), then responsible for runtime operations, announced termination of service on 31st March 2000[13] in accordance with the Marine Navigation Plan to 2015. Decca was used around the world, most prominently in Japan and Canada although the former deployment was superseded in 2000.

Master stations transmitted continuous sinusoids at 2 kW on well-known frequencies in 70–130 kHz (wavelengths about 1 mile)[18]. Synchronized slaves radiated energy on characteristic, published (non-unity) multiples of the master frequency from masts distant 60–100 statute miles from the master and erected to form rough 120° angles, a geometry advantageous for error performance. Figure 2.2 illustrates the relative geometry of a typical "coloured" master/slave set used in northern Germany. Receivers sets contained a three (or more) channel radio receiver, an analogue multiplier and phase comparison circuitry. By monitoring the changing phase differences an offset in the horizontal plane from a fixed epoch could be computed. Decca provided only *relative* changes in position, never an absolute fix. Phase measurements did not uniquely determine position offsets; the power supply to a Decca Navigator receiver was continuous because position ambiguities could only be resolved in the context of the recent location and heading of the vessel.

Initially L-series charts—hydrographer's maps overlaid with hyperbolic Decca lattices (contours of constant phase difference)—were used for fixing and navigation. Automatic clock-dial "decometers" spared the operator from manually observing signals on an oscilloscope and reduced the latency of obtaining fixes compared with Gee. HARCO (hyperbolic area coverage) units were early digital interface circuits designed to compute rectilinear co-ordinates from the raw Decca output and transfer these data to a computer[18]. More recently yachts were equipped with digital receivers which, once calibrated in a known location, provided a continuous readout on an LCD display or digital map of the vessel's current position, expressed

Table 2.2: Prevalent error sources in the BGLA Decca Navigator Service (1939)

Power supply fluctuations	Brief interruptions, abrupt changes in phase and frequency drift of the transmitters' mains power supplies caused phase shifts in the radiated signals which lead to arbitrary magnitude positioning errors undetectable to the navigator.
Antenna damage	Physical damage to the transmitter aerial may cause confusing, strong secondary harmonics and lessened range.
Atmospherics and interference	Ground and sky wave interference hindered successful interpretation of the signals and varied in significance between negligible and severe hour-by-hour and with day/night (the sky wave channel opens at night). Meteorological conditions affected the reflection altitude and the proportion of incident energy reflected back to the surface.
Rain showers	Absorption increases path attenuation and reduces range, and a scattering effect reduces precision.

Table 2.3: Drawbacks of WJ O'Brien's Decca Navigator Hyperbolic Radio Navaid (1939)

Dense infrastructure	In order to maintain reliable synchronization with the master base lines could not exceed 100 miles. Consequently Decca had a heavy infrastructural requirement.
Limited range	The useful service radius was (at best) 200 miles and inadequate for many excursions.
Spectrum inefficiency	Each master and slave station was allocated a unique portion of the frequency spectrum, and stations were numerous.
Undetectable errors	Many sources of error were undetectable to the navigator who was, therefore, unaware that using another station set would improve accuracy.

as ecliptic longitude and latitude. Raymarine Ltd manufacture units offering the same information digitally via a proprietary SeaTalk[1] bus: a 3-wire, multi-drop, distributed-OR, simplex power and data network supporting multiple masters through carrier sense, back-off and probabilistic collision avoidance without central arbitration.

Decca Navigator was more accurate than Gee although initially less reliable. 7 m accuracy was reproducible with good probability near the baselines, degrading to 1–2 miles at 200 miles range. The prevalent factors affecting user position errors are described in Table 2.2 and the drawbacks described in Table 2.3. Announcements of defective transmitters and exceptionally severe meteorological interference were made as spoken word over a radio channel through the Channel Navigation Information Service (CNIS)[14] when, if left unaccounted, lane slippage would have occurred. The automatic receivers were unable to exploit these intimations without human intervention.

2.4   OMEGA

OMEGA was a worldwide very low frequency (VLF) hyperbolic radio navigation system established by the United States Navy with international co-operation. Two decades of research and background work culminated in the expensive construction of eight 1200 ft transmission towers in 6 countries intended to

---

[1] SeaTalk is a registered trademark of Raymarine Ltd, Anchorage Park, Portsmouth, Hampshire, PO3 5TD; trademark 1423542.

provide repeatable location precision of 4 nautical miles for global oceanic military air traffic although significant use was confined to civilian users. The operating frequencies were changed repeatedly during the lifetime of OMEGA but remained in 10–12 kHz band[14]. Each transmitter continually radiated a pulsed code at 10 kW and an identification code on a unique station-specific carrier frequency. Codes repeated at intervals of 10 seconds, consequently independent position fixes were available at the same rate. Synchronization between stations was initially established using matched, stable oscillators and later with atomic reference clocks at each site. Initial operating capacity was reached in 1983.

Hyperbolic lines of constant code phase offset between the transmissions from any pair defined lanes which had width 8 nautical miles when VLF is used. Navigators operating single frequency receiving apparatus were required to supply their starting location accurate to 4 nautical miles; 144 nautical miles accuracy sufficed to eliminate ambiguity for multichannel receivers. Navigators counted the crossings of lane boundaries to determine their offset from the initial position, accurate to 4 nautical miles. It was also possible to operate a similar technique to Gee and Decca: intersecting lines of position on hydrographer's charts.

Global service availability was 97%, including scheduled maintenance which was announced 30 days in advance. Sources of user error included counting errors caused by radio nulls, reduced power transmissions and echoes: often eliminated by dead reckoning or inertial navigation. Ionospheric disturbances gave rise to random errors of 0.8–1.6 nautical miles most prominent at local twilight and lead to lane slippage. Absorption of charged particles near the magnetic poles caused 0.8–4.0 nautical miles errors. Rain showers distorted radio transmissions and lead to lane slippage.

OMEGA was finally shutdown at precisely 0300 GMT on 30th September 1997.

2.5 LORAN

Standard Long Range Navigation (LORAN) is a pulsed hyperbolic radio navigation system designed specifically for navigation at sea level over water and as such the transmitters are located on exposed coastal promontories. Loran provides absolute fixes independent of external cues at greater range over water than Decca but to lower accuracy. Transmitters operate in 1700–2000 kHz band and radiate approximately 100 kW. Propagation of electromagnetic radiation at these frequencies is dictated by soil characteristics and ionosphere activity. The initial 1940 deployment was formulated by the Microwave Committee then chaired by AL Loomis and co-ordinated by Bell Labs (New York). Receivers rely on ground waves during the day but a sky wave channel, open only at night, can be used for lower precision navigation over very extended distances (Table 2.4). Timing errors decrease in significance with increasing distance from the base line and partially compensate increasing geometric errors. Nocturnal sky wave navigation offers similar accuracy to Celestial Navigation and is available in all but the most severe weather conditions. Signal strength is invariant with altitude except for ground waves over land when the greatest variations occur in the lowest few thousand feet.

Pulse lengths of 50 μs are used to limit spectrum use although shorter pulses could provide greater timing precision and thus improved accuracy. Concurrent use by several transmitters of the same frequency further enhances spectral efficiency; characteristic identification pulses distinguish superposed transmissions.

Table 2.4: Propagation range of Standard LORAN transmissions

Day	Over Sea	700 nautical miles	Ground wave channel
Day	Over Land (surface)	100 nautical miles	Ground wave channel
Day	Over Land (aircraft)	250 nautical miles	Ground wave channel
Night	Over Sea	500 nautical miles	Ground wave channel
Night	Over Sea	1400 nautical miles	Sky wave channel

Table 2.5: Physical sources of error in Skywave Synchronized (SS) LORAN

Imperfect skywave synchronism	Errors in the skywave path compensation factors caused by the changing altitude of the E-layer ionosphere lead to errors in station synchronism and thus user fix errors.
Skywave accuracy	Errors change in significance across the coverage area.
Free electron clouds	Clouds of free electrons caused by corpuscular bombardment of the atmosphere by particles ejected from the sun alter channel characteristics. Their appearance is most common at high latitudes, during the summer months, and at maxima of the sunspot activity cycle. Their presence is sporadic in space and time, by day and night and exist for a few minutes to several hours. Each cloud appears at a very constant height and can be several hundred miles in diameter. They may move slowly or at very considerable speed. Ionisation density is usually low but is occasionally very high.
Magnetic activity	Corpuscular bombardment as above also affects the freer electrons found in the F-region ionosphere. SS-LORAN stations fall out of synchronism; their service is degraded and available for reduced hours, as skywave propagation is appreciably lessened by increased altitude of the F-region and rarefied ionisation.

Loran receivers most commonly used three stations in two pairs to fix position. Three or more lines were available at greater range and could be used to increase precision and provide an estimate of error: Goudsmit shows that the probability of a true position falling inside the triangle formed by three independent lines of position is 1-in-4.

2.5.1 SS-LORAN

Skywave-Synchronized LORAN (SS-LORAN) is a night-time-only augmentation to Standard LORAN which exploits the large nocturnal range of E-layer (lower altitude) ionosphere reflections to extend the base lines to 1200–1300 miles and thus improve geometric accuracy. Physical sources of error are explained in Table 2.5.

An extension to the initial LORAN deployment covered the North Atlantic Ocean using 4 SS-LORAN transmitters at the corners of a rough square. Geometric advantage results because lines of position intersect forming angles of $60°$ or more over more than one million square miles: user fix uncertainty is uniform—0.9 nautical miles—tending only to 1.7 nautical miles very close to the corners. Greatest error occurs during ionosphere storms which occur 1% of the operational time and cause errors of 5–6 nautical miles. The skywave channel suffices to maintain station synchronization 99.8% of serviceable hours except in auroral zones where charged particles are deflected through the atmosphere by the Earth's magnetic field.

2.5.2   LF-LORAN

Low Frequency LORAN (LF-LORAN) increases daytime propagation range to the distances offered by nocturnal Standard LORAN. 300 μs pulses are required but the longer duration reduces timing precision to 4 μs. LF radiation never penetrates beyond the ionosphere E-layer: consequently there are no trains of reflected pulses which complicate night-time use of other LORAN networks. LF-LORAN transmitter stations are more complex and slaves often run on the same frequency, requiring additional identification pulses.

2.5.3   Analysis of LORAN User Fix Error

Figure 2.3 illustrates a typical position fix using hyperbolae Q and R. The reported position is C and contours in the probability space associated with the receiver's actual position are elliptical shells centred on C and inclined at angle Ω to the co-ordinate x-axis. The semi-major and semi-minor axis lengths depend on transmit power levels and the desired probability of the receiver's true position falling within the perimeter. Analytic expressions characterising 50% and 90% probability ellipses for LORAN power levels are shown in Figure 2.4. Probability parallelograms with edges parallel to the chart lattice lines are often used to approximate probability ellipses because their dimensions can be determined without computational assistance, for example, at 50%:

$$\text{length parallel to Q} = 3.12 p_2 \csc \Phi \tag{2.1}$$

$$\text{length parallel to R} = 3.12 p_1 \csc \Phi \tag{2.2}$$

$$\text{length diagonals} = 3.12 \csc \Phi \cdot \sqrt{p_1^2 + p_2^2 \pm 2 p_1 p_2 \cos \Phi} \tag{2.3}$$

where p_1, p_2 are as defined in Figure 2.4 and Φ is the acute intersection angle between hyperbolae Q and R.

2.6   Post Office Positioning Indicator

The British Post Office Positioning Indicator (POPI) used four vertical antennae forming an equilateral triangle with a central mast as shown in Figure 2.5. The operating frequency radiated from the perimeter antennae in rotation at 5 cycles per second with a space (indicated by an underscore) between repetitions. Thus three sets of confocal hyperbolae, focused on the antennae are formed in phase difference space which, at sufficient distance, appear to an observer indistinguishable from a set of straight lines diverging from the midpoint. The frequency of a continuous, steady omnicast from the central transmitter was chosen to beat in the (human) audible spectrum with the perimeter signals depending on their phase difference, which was indicated on a meter. A position fix was established by repeating for a second fixed ground station and applying standard TDOA techniques. Because two signals from each basestation were used and each travelled almost equal distance to the other, ionospheric effects delayed the signals equally and this source of error was largely eliminated.
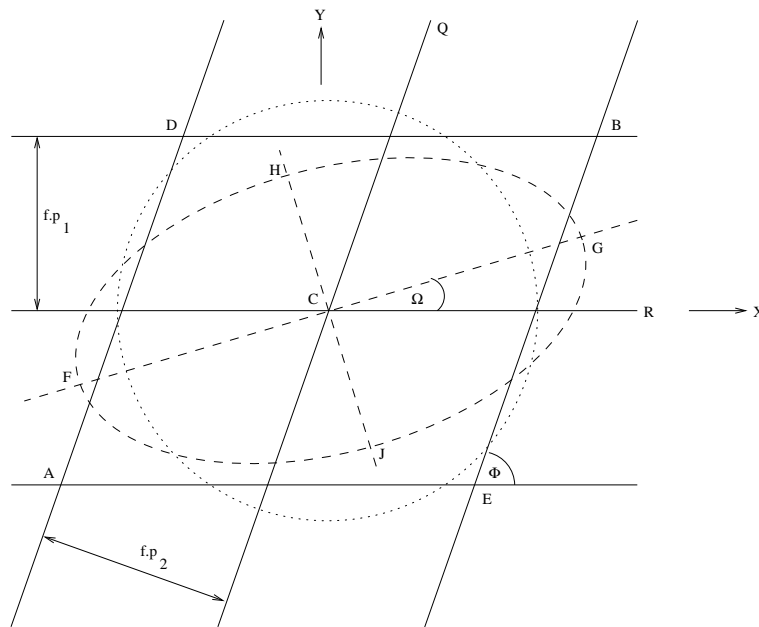
Figure 2.3: Probability Ellipse and approximating Probability Parallelogram

2.7   Orfordness Beacon

The British Orfordness Beacon provided a means for World War II pilots to determine their heading using a radio receiver, a timepiece and the signal emitted by a single, fixed ground station. The ground station continuously radiated a steady tone through a vertically polarised loop antenna rotating at precisely 1 revolution per minute about its vertical axis. Two null radii in the polarisation pattern thus swept around the beacon at $6°$ per second and a coded interruption was given each revolution as one passed through north. The observer measures the time difference, Δt, in seconds between hearing the coded interruption and observing a null radius at their position. The azimuth of the observer, Z, is given by

$$Z = 6 * \Delta t \tag{2.9}$$

or this plus $180°$, an ambiguity easily resolved by pilots given their context. Clearly the error in bearing is directly proportional to any error in Δt. When variation is permitted the navigator must know of the station in use whether north calibration is true or magnetic. Unless maintained at zero tables of the asymmetry coefficient, the values of the north mark offset azimuth, rotation rate offset, and the drifts in these quantities are required by the observer. Variation in expected precision across the service area is a function of range, the breadth of the null radii as determined by the quality of the antenna construction, and interference.

2.8   Sonne

Sonne was a complex German relative bearing discovery system reliant on a ground station emitting three signals with range 250–500 km via three, fixed, colinear, vertical antennae. An interference pattern comprising 12 sectors was created by suitably spacing the antenna and keying and phasing the signals. Pulses

With reference to Figure 2.3...

Let T' and T'' be the time differences of arrival, obtained at the same location from two pairs of stations. Further, let the errors in these two measurements be T_1 and T_2 respectively. The receiver's true location is thus at perpendicular distances $p' = k\omega_1 (T_1 - T')$ from Q and $p'' = k\omega_1 (T_2 - T'')$ from R where ω is a factor of geometric precision and k a constant depending on the unit of length:

$$k\omega = \begin{cases} 0.08086 \csc(\Psi/2) & \text{nautical miles per } \mu\text{s;} \\ 0.09311 \csc(\Psi/2) & \text{statute miles per } \mu\text{s;} \\ 0.14985 \csc(\Psi/2) & \text{km per } \mu\text{s;} \\ 491.62 \csc(\Psi/2) & \text{ft per } \mu\text{s.} \end{cases} \tag{2.4}$$

where Ψ is the angle between the two directions from the observer to the transmitters.

Assuming the errors affecting T' and T'' are independent and normally distributed, they have standard deviations $\sigma_1 = \sqrt{\sum \frac{(T'-T_1)^2}{n_1}}$ and $\sigma_2 = \sqrt{\sum \frac{(T''-T_2)^2}{n_2}}$ made over large numbers of observations, n. Distances p' and p'' have standard deviations $s_1 = k\omega_1\sigma_1$ and $s_2 = k\omega_2\sigma_2$. Let probable errors p_1 and p_2 be

$$p_1 = 0.6745 s_1 \qquad p_2 = 0.6745 s_2 \tag{2.5}$$

Let Ω be the angle between the semi-major axis of probability ellipse FG/HJ and the x-axis as shown in the Figure. Ω can be computed from

$$\tan 2\Omega = \frac{2p_1^2 \cot \Phi}{p_1^2 (\cot^2 \Phi - 1) + p_2^2 (\cot^2 \Phi + 1)} \tag{2.6}$$

and let α and γ be defined as

$$\alpha = \sqrt{\frac{1}{2} (p_1^2 + p_2^2) \csc^2 \Phi + p_1^2 \cot \Phi \csc 2\Omega} \tag{2.7}$$

$$\gamma = \sqrt{\frac{1}{2} (p_1^2 + p_2^2) \csc^2 \Phi - p_1^2 \cot \Phi \csc 2\Omega} \tag{2.8}$$

Now, a 50% probability ellipse, inclined at Ω to the x-axis has semi-axis lengths $FG = 3.49\alpha$ and $HJ = 3.49\gamma$. A 90% ellipse has the same inclination but dimensions scaled by 1.82.

Figure 2.4: Analytic description of shells of probability for LORAN fix errors
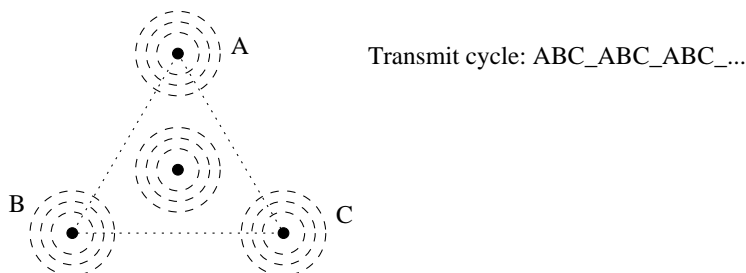
Figure 2.5: Plan of the Post Office Positioning System

of dots were heard in odd sectors and dashes in interleaving even sectors while equisignal (unbroken tone) was heard on sector boundary radii. The signals broadcast by the outer antennae were shifted in phase so the interference pattern rotated smoothly through one sector in 60 seconds. An equal period of omnidirectional, continuous tone from the central transmitter followed before the interference pattern was re-established and rotated exactly as in the previous cycle.

Navigators measured time from the beginning of a cycle to the equisignal radii sweeping through their position. It was assumed the navigator knew by some external means which sector he occupied—typically conventional direction finding or dead reckoning—thus providing sufficient information to determine a relative bearing from the station.

Chapter 3

Satellite Timing and Ranging

Following the launch of Sputnik I on 4th October 1957, a 184 lbs Russian artificial earth satellite, American physicists Guier and Weiffenbach at the Applied Physics Laboratory (APL) analysed the vessel's radio transmissions using digital computers[19]. They determined the orbit parameters using only single-pass horizon-to-horizon Doppler measurements from the 20 MHz unmodulated broadcast carrier. Their superior, McClure, suggested working on the *Inverse Problem* or *Navigation Problem* as it was later known: positioning the receiver station given precise orbital models. A 50-page proposal was put to the United States Navy Bureau of Ordnance.

3.1   TRANSIT

The Navy Navigation Satellite System, known as TRANSIT, was funded by Advanced Research Projects Agency (ARPA) in 1958 and assigned to the United States Navy in 1959[19]. The first launch—Transit 1A—from Cape Canaveral Air Station (Florida, USA) using an Able upper stage and Thor booster on 17th September 1959 was unsuccessful. A second attempt on 13th April 1960 using an Ablestar upper stage successfully placed Transit 1B in polar orbit after a pioneering in-space engine restart manoeuvre. Subsequent launches deployed additional satellites into the Transit 1 orbital path and populated a second polar orbital, Transit 2. Initial operating capacity (IOC) was reached in 1964 and full operating capacity (FOC) in October 1968. Civilians were granted access in 1967.

The constellation of 3 operational satellites and 3 "stored-in-orbit" spares was composed of 110 lbs Oscar and later 350 lbs Nova satellites in nominal 600 nautical mile (1100 km) orbits. The control system constituted 3 globespanning monitoring stations and was responsible for uploading corrections and firing thrusters to maintain approximately equal orbital spacing and minimise the greatest period between availability around the globe—the system was never continuously available anywhere on the surface of the earth. The satellites transmitted orbit ephemerides on 150 MHz and 400 MHz carriers. Ionospheric delay to propagating electromagnetic radiation, the most significant physical error source, is inversely proportional to the square of frequency so dual-frequency receivers can estimate and correct for ionospheric effects. Although the stated goal was to achieve an initial accuracy of 0.5 nautical miles (926 m), early navigators were plagued by errors of 1–2 km in their geoid models. 13 ground stations were used to collect Doppler

measurements and many months of computer time on the APL IBM7094 computer were consumed in calculations to update the geodetic model of terrestrial gravitational nonuniformity. Armed with updated models, Navy vessels could reliably and repeatably pinpoint their location with error less than 0.1 nautical miles (185 m). Co-operating receivers could be used to determine the relative positions of two objects with less than 10 metres error.

A TRANSIT receiver provides 2-dimensional position fixes sufficient for most offshore Naval operations and adequate to correct accumulated drift in Inertial Navigation systems when required. Only one satellite was required to compute a fix.

The navigation transmissions were intentionally disabled on 31st December 1996 when the Federal Radionavigation Plan (FRP) declared GPS (Section 3.2) would be used alone for military timing and ranging. The space vehicles achieved an average lifetime of 12 years, most eventually succumbing to power supply failures. Orbital positioning was not maintained for a period prior to final termination of service and periods of unavailability extended to 6 hours in the worst case.

The development of TRANSIT advanced the sciences of space, geodetics, terrestrial orbits and atmospheric effects. Deeper understanding of these issues facilitated the development of the contemporary Global Position System (GPS). Table 3.1 summarises the TRANSIT system.

Table 3.1: Summary of TRANSIT

TRANSIT—Navy Navigation Satellite System	
Availability	All weather, global. Initially available every 1–3 hours; satellite in view for approximately 20 minutes. Later temporal availability varied as satellite orbits became highly unevenly spaced.
Orbit	1100 km—low orbit susceptible to atmospheric drag and local gravity nonuniformities were very significant to orbit. Geodetics were improved in 1960s in order to be able to achieve acceptable positioning accuracy.
Radio	150 MHz and 400 MHz carriers are affected by ionospheric delay and random disturbances more than higher frequencies.

3.2   NAVSTAR GPS

The Navigation Satellite Timing and Ranging (NAVSTAR) Global Positioning System (GPS) is a United States Department of Defense (USDoD) project providing 24-hour, all-weather timing, navigation, and surveying worldwide to an unlimited number of users and is estimated to have cost US$ 8–10 billion[47, 19]. The program of space vehicle (SV) deployments began in 1978 with the launch of the first 1860 lbs Block I (testing/development) satellite and IOC was announced on 8th December 1993 when 24 SVs were simultaneously operating in Blocks I, II and IIA (operations). FOC was defined to occur when 24 simultaneously operating SVs from Blocks II and IIA were in service.

GPS SVs avoid atmospheric drag in high altitude, low eccentricity elliptical orbits of semimajor axis 26 000 km. Orbits are described using a set of six osculating Kepler elements[19]. Block I SVs orbit

at inclination 63°; Block II and IIA orbits have inclination 55°. The orbital period is 11 hrs 56 mins: the right ascensions of the ascending nodes regress slightly with each revolution. Table 3.2 explains the orbit corrections terms needed to achieve precise navigation on/near the earth surface.

Table 3.2: Orbit correction factors for GPS Space Vehicles

NAVSTAR GPS	
Correction	*Description*
Nonuniform terrestrial gravitation	The models developed for TRANSIT no longer afford the accuracy required. GPS parameters are derived using gravitational models of the earth with non-rigid (viscous liquid) cores and an elastic ellipsoid earth.
Lunisolar Precession of the Celestial Ephemeris Pole (CEP) and Nutation	Precession and nutation of the earth about its spin axis arise because the earth is neither spherical nor of uniform density. 106-term numeric models are in widespread use describing oscillations of varying amplitudes and periods from 18.6 years to 5 days. Figure 3.1 plots polar precession and nutation between 1993 and 2000; the general leftward drift—*Polar Wander*—is currently without scientific explanation.
External gravitation	**The sun**: topocentric acceleration caused by the very significant mass of the sun compared to that of the earth (332946.0 times) perturbs SV orbits. **The moon**: a similar correction is required due to immediate proximity (rather than its relative mass of 0.0123002 that of the earth).
Solar Radiation Pressure (SRP)	Photons emitted by the sun strike the illuminated surfaces of the SVs causing an acceleration which, if left unaccounted, amounts to 1000 m in 1–2 weeks. The effect depends on the effective illuminated area, surface reflectivity, luminosity of the sun and distance from the sun. The ROCK4 (Block I) and ROCK42 (Block II) SV structure models are used to approximate SRP effects and the *Y-bias* term describes thermal phenomena and misalignment of the SV or its $7.2m^2$ solar arrays. SRP is zero when the SV lies hidden in the earth's shadow; biannual eclipse corrections are required as each SV passes through the earth's umbra (SRP is 0) and penumbra (SRP changing). Figure 3.2 illustrates.
Lithosphere tectonics	The tectonic plates which make up the surface of the earth move slowly and occasionally abruptly. Relative positioning of co-operating receivers is used to quantise the shifts caused by earthquakes.

3.3   GLONASS

The Russian Global Navigation Satellite System (GLONASS) operates similarly to GPS. Each satellite transmits on a unique frequency rather than with a unique CDMA near-orthogonal code. For brevity, interested readers are referred to the abundant literature available on GLONASS.

Polar Motion 1993--2000 (with errorbars)
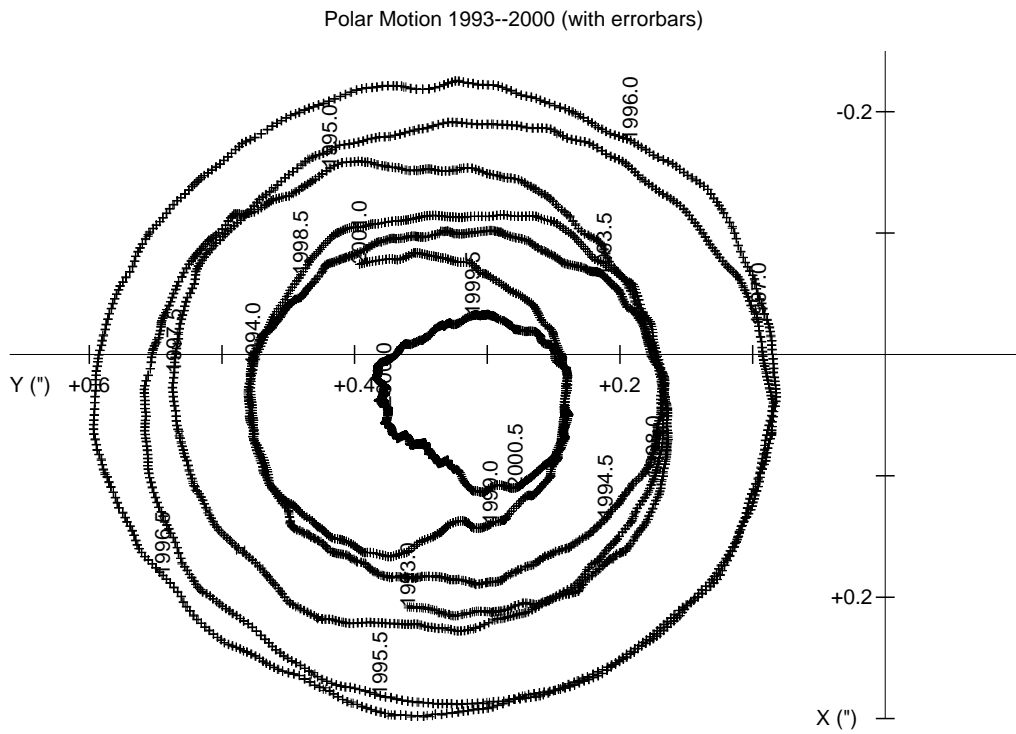
Figure 3.1: Terrestrial precession and nutation 1993–2000
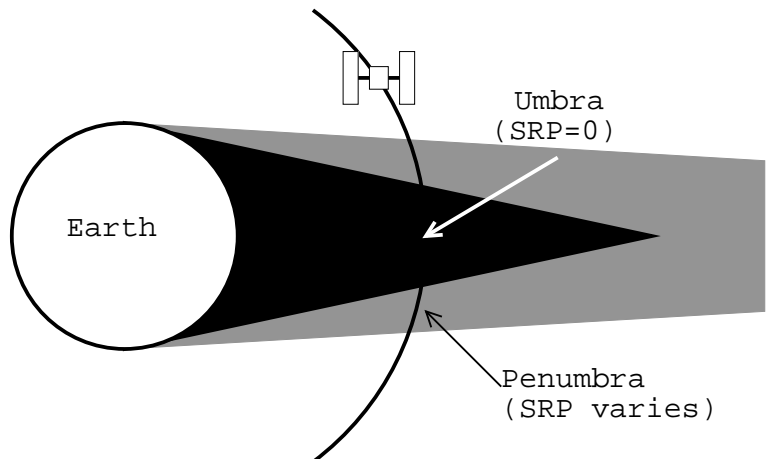
Figure 3.2: Ecliptic variation in SRP on orbiting GPS satellites

3.4   Galileo

At the time of writing the European Union have plans to develop a satellite timing and ranging system capable, amongst military and commercial goals, of replacing current air-traffic and airport location systems. Plans continue to change; suggestions have included deploying new space vehicles and the cheaper alternative of combining signals from GPS and GLONASS. The error properties of the latter technique require very sophisticated analysis.

Chapter 4

Outdoor Location Systems

4.1   Road Traffic Location Systems

Third party vehicle equipment manufacturers, most notably Tracker, use terrestrial radio to locate fleet and stolen vehicles using familiar techniques. Congestion monitoring systems however exemplify additional technologies.

Traffic*master* affixed to motorway bridges in the UK an initial network of infrared transceivers which captured the speed of passing vehicles by accurately measuring Doppler shift on reflected waves. The tracked entities are anonymous traffic queues, not individual vehicles. When flow rates fall below 30 mph congestion reports are generated and transmitted to a central control facility. Sensor IDs are resolved using a deployment database to Cartesian OSGB co-ordinates, roadnames, the nearest junction and the direction of traffic flow to express locations in congestion reports. Sensor reliability and accuracy are good except in heavy snow. Location errors are constant with time and depend on the initial survey and the presence of any errors in the resolution database. Doppler sensors detect congestion events only when a tailback has reached the upstream sensor: there is inherent latency in report generation which varies across the country with deployment density. Doppler detectors cannot detect stationary vehicles unless augmented with range-finding radar.

The sensor network was aggrandised and coverage extended to trunk and A roads with visual light cameras

Figure 4.1: A Traffic*master* visual light camera installation (A14 J35, Cambridgeshire)

Figure 4.2: Traffic*master*UK network coverage (2002). Reproduced with permission.

annexed to bridges above the central lane of 3 lane roads and the overtaking lane of 2 lane roads (Figure 4.1). Image processing on site locates number plates in stills and the central four characters are identified using optical character recognition (OCR). Electronic 'tags' representing these digits are timestamped and communicated through the pager network to a central control facility where passive target flow measurement (PTFM) algorithms compare the timestamps of large numbers of vehicles passing adjacent cameras to determine average vehicle speeds. Road flow heuristics improve the controller's model of the state of the road network and reduce the update latency. Locations are expressed in a format suitable for humans with local knowledge or a streetmap: road sections and direction of travel, for example "A14 J33–J32 westbound."

Figure 4.2 illustrates the Traffic*master* sensor availability. The network extends into mainland Europe where it is especially well developed in Germany.

Figure 4.3: A magnetometer induction loop detector buried in a sawn groove in the tarmac and grouted with sealant
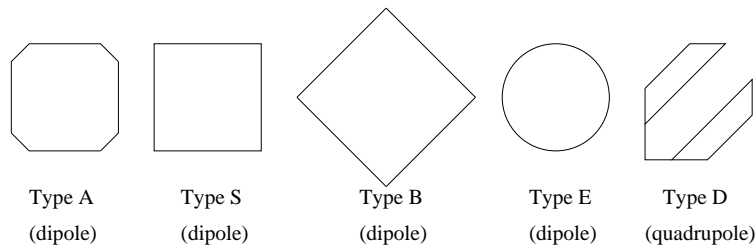

Type A	Type S	Type B	Type E	Type D
(dipole)	(dipole)	(dipole)	(dipole)	(quadrupole)

Figure 4.4: Loop morphologies from Santa Clara signalised intersections

4.2   Magnetometer Detectors

Traffic engineers specify magnetometer detectors to collect highway flow statistics and control dynamic traffic light timings by adjusting the red- and green-times in response to changing traffic conditions. Induction magnetometers (IM) actively excite a coil to measure changes in inductance of less than 0.01% caused by the presence of iron-containing steel alloys. Typically 3–5 turns per coil are used and three coils are deployed 10–30 metres from an intersection. IM loops are unable to detect stationary vehicles. Figure 4.3 shows the head loop (closest to crossing) of three skewed parallelogram detectors used control a pedestrian crossing on Yarrow Road, Cambridge (OSGB: 549470 E $\pm$ 10m, 256580 N $\pm$ 10m).

Maki and Marshall analysed the performance of different loop morphologies used by Caltrans[1] in Santa Clara County, USA, in [29] (Figure 4.4). Types A and E, which contain no damage-prone acute angles, are the most widely installed in California and construct dipole fields suitable for detecting passenger cars and trucks up to 0.6 m from the cable with minimal interlane spillover. However, Wachtel reported that detection of high-body sports and haulage vehicles is poor when the coils are operated at sensitivities which reject spillover[49]. Wachtel further demonstrated that A and E coils are unable to detect bicycles in their centres (because the magnetic flux is there in the plane of cyclists) and reports on designs by Aggarwal, Hamm and Woods, and Duemmel which give low spillover but incorporate turns oblique to the traffic flow to detect vehicles across the width of the lane.

Dual-axis fluxgate magnetometers sense changes in the horizontal and vertical components of the Earth's magnetic field caused by proximate ferrous objects. The sensors are passive and able to detect stationary vehicles.

---

[1]California State Department of Transport

The location accuracy of magnetometer detectors varies with loop morphology and between models of vehicle; errors exceeding 1 m are rare and generally attributable to vehicles straddling two lanes. Detection events are naturally sporadic in space because a network of loops has scattered pinpoint availability. Sightings are anonymous—individuals cannot be reliably identified from the total population of registered vehicles—but vehicle classification based on time signature analysis of the loop inductance waveform is often possible. Loop cables grouted with rubber sealant into grooves sawn in the tarmac are reliable and capable of withstanding prolonged climatic and physical load cycling. Loops are occasionally adhered to the surface but damage caused by passing traffic, street sweepers, and snow ploughs reduces their operational lifetime and reliability.

A reliability study of detectors on a section of California interstate found the detection error rate to be one per hour per detector in rush hours. The modal errors were:

- double triggering of the thresholder by long trucks; and

- missed vehicles caused by lane changing while passing the detector.

Magnetometer detectors are capable of direct velocity measurement (speed and crude direction) but statistics scientifically valid for traffic monitoring are often obtained through comparing the outputs of several detectors laid as a speed trap. The first time derivative of detections—flow rate or density—is the basis of intelligent transportation system (ITS) research and is often present in databases and logs despite its functional dependence on a sensed quantity.

4.3   Infrared Detection

Passive infrared (PIR) receivers compliment Traffic*master*'s active approach. PIR sensors detect changes in emitted or reflected energy caused by vehicles passing through the target area. Long wavelength infrared energy is attenuated less by rain, snow, and fog than is visible light. PIR detectors offer potentially improved performance in inclement weather and are widely used in military and security applications. Detectors are not affected by sun glint, headlight glare, or shadows and operate equally at night and during the day.

Range finding is also used to detect vehicles. Pulses of energy are emitted by a low power laser and the time taken by reflections to return to a detector is measured. The presence of a vehicle in the sensed area is detected by a reduction in the path length. Active IR range finding is able to detect stationary vehicles but detection of motorbikes, mopeds and bicycles is unreliable. Vehicles can be classified based on roof height but individual identification is impossible.

At the instant of detection, vehicle locations are known very precisely along the direction of travel. The uncertainty in the perpendicular component is equal to the width of the vehicle.

4.4   Ultrasonic and Passive Acoustic Techniques

Vehicle engines and transmission trains emit characteristic longitudinal pressure waves at ultrasonic frequencies. Passive ultrasound receivers are used to detect the presence of vehicles. Lane separation is

Table 4.1: Image processing difficulties arising from unconstrained environments

fog and mist	precipitation
airborne pollutants	dirt and frost on the lens
low ambient light	low sun angle (winter months)
reflections	shadowing
partial and total occlusion	glare (glass and wet surfaces)
low interclass variation, e.g. mopeds and pedestrians	

difficult to achieve so positioning uncertainty is at least the width of the road. Loud trucks and poorly maintained vehicles trigger thresholding circuitry farther from the detector than do softer emitters. Strong winds, heavy snowfall, and precipitation also limit accuracy.

Active sensors are also used to detect vehicles using timed pulse reflections and compute speeds (of moving vehicles) from Doppler measurements of a continuous carrier. Each is affected by weather conditions as above and pulsed emitters are unable to reliably detect fast moving vehicles.

4.5 Visual Light Camera Monitoring

Visual light cameras are potentially cost-effective vehicle, pedestrian and incident location technologies as no infrastructure other than a passive camera secured to a fixed mounting is required. State of the art research systems monitoring intersections perform adaptive background separation followed by image segmentation and macrotemporal blob tracking. Maurin, Masoud, and Papanikolopoulos require no programmed knowledge of the road geometry provided the camera position and orientation are chosen to meet shadow and glare minimisation criteria[30]. Others uses *a priori* knowledge of intersection layouts to allow real-time 3-dimensional scene reconstruction and occlusion tracking.

The unconstrained nature of outdoor environments creates unamenable difficulties for image processing algorithms which increase location errors and reduce detection reliability and system availability (Table 4.1). The use of multiple cameras, either as alternative viewpoints or in stereoscopic combination, is often considerably beneficial but installations are bespoke and a generally applicable solution remains a research goal.

Object locations generated using a world model from monocular images are typically accurate only to the width of the object or length of shadows. Oertel, Dimter, and Szoska use registration of images taken simultaneously by calibrated stereo cameras to find the depth of objects in the scene and reject glare and shadows before performing image segmentation[36]. Location resolution is usually sharpest near the camera and decreases linearly with distance due to the pixelation granularity of the camera's charge coupled device (CCD) array.

Visual light intersection monitoring is used to seed traffic models in Paramics simulations for road network studies. Veeraraghavan, Masoud, and Nikolaos Papanikolopoulos are working to identify collisions and near misses to facilitate the improvement of hazardous intersection designs[48]. Oertel, Dimter, and Szoska, also motivated by safety, seek to arrest surface and underground trains entering stations in the presence of platform or track hazards[36].

4.6   Radio Frequency Identification—RFID

An RFID transponder embodies a uniquely allocated serial number. Transponders were initially encased in biomedical glass and subdermally implanted in ferrets to assist locating the mammals when foraging in rabbit holes. Texas Instruments hold many of the earliest patents implemented in the TIRIS[2] brand and the plurality of RFID-based patents since the 1980s confirm industry's leading rôle: printable antennae and conductive ink[35], smart postage stamps[46], cattle auctions[16], tracking/diagnosing network assets[31], identifying golf balls[7] and Black Jack card game training[37]. The US railroad industry encouraged early developments to track cargo wagons because RFID penetrated the rain, snow, fog, and dirt which plagued previous near-visual light barcode readers. Identronix and Amtech developed 900 MHz and 900/1800 MHz and large semiconductor manufacturers, notably Texas Instruments and Philips Semiconductor, commercialised very low frequency (VLF), low frequency (LF), medium frequency (MF), very high frequency (VHF) and ultra high frequency (UHF) versions in 1983. These transponders were write-once, read-many (WORM) and programmed during manufacture, later versions allowed one-time programming of the serial number after manufacture.

Most transponders were battery powered until the (US) automotive industry innerved the development of passive transponders capable of surviving thermal exposure in paint ovens. The capacity of the communications channel was 250 Kbit/sec and amplitude modulation, 1-of-16 pulse position modulation (100% depth) and frequency shift keying at the physical layer supported two link-layer protocols: tag-talks-first (TTF) and interrogator-talks-first (ITF). The tag response signal strength varies with distance, d, as $1/d^4$ for passive tags and $1/d^2$ for active devices. Tags with up to 8 Kbits of user-reprogrammable memory became possible in the late 1990s with advances in embedded memory technologies. Ferroelectric memories are amenable to integration with logic on a single silicon die and consume three orders of magnitude less power on average than other refresh-less technologies[3] with durability 100 000 writes[44]. The activation energy required to transmit accumulates as charge stored in a capacitor until sufficient to sustain a backscattered transmission. The transponder coil is shunted through a transistor and transformer-like properties of the RF link cause fluctuations of approximately 100 mV on a 100 V sine wave in the field generator. A colocated demodulator decoded the binary sequence and verified packet CRC-16 checksums[4].

Contemporary transponders embedded in polyvinyl chloride (PVC) mouldings offer a rigid construction and flexible inlays are also available. The International Organization for Standardization (ISO) promoted interoperability of *vicinity cards*.

4.6.1   ISO 14443/15693

Transponders are energised by a 13.56 MHz RF field generator; communication occurs in the same band using ITF. Multicast (inventory) commands affect each proximate tag while unicast addressing is achieved through the unique transponder identification number impressed into the read-only data segment. ISO 14443 devices support block-wise commands to access read-only and read-write address spaces[25, 26]. An anticollision/transmission protocol prevents data-destructive interference between transponders while main-

---

[2]TIRIS is a registered trademark of Texas Instruments Holland B.V., number 1363072

[3]ferroelectric write operations consume 1 μJ for reads and writes—significantly less than EEPROMs and Flash for writes, rather more for reads

[4]the Consultative Committee for International Telegraph and Telephone (CCITT) polynomial is used

taining a read-rate of approximately 50 commands per second per RF zone[27, 28]. ISO 15693, a higher data-rate specification was standardised in 2000/2001[21, 22, 23]. The UK Radiocommunications Agency (RA) stipulate a maximum radiated level of 42 dBμA/m at 10 m for unlicensed operators[2], equating to read/write distances of about 500/250 mm with unsophisticated antennae.

4.6.2   RFID Location

ISO 15693 cards activate in approximately 95 dBμA/m RF fields. Interrogators designed for access control systems attain this flux density within conical regions extending 100 mm perpendicular to the plane of a single turn, copper-track antenna circumnavigating the circuit board[5]. Detection implies the location of the tag is within the region bounded by a 95 dBμA/m contour. The continued presence of tag is confirmed by inventorising the RF zone repeatedly; the absence of a tag's ID in interrogator responses is assumed to imply the tag lies outside the activation zone although pathological orientations of 2-dimensional coils in the RF field reduce the coil/field flux linkage and activation energisation is not reached.

4.7   Laser Ranging

Laser ranging devices operate by firing low or high power lasers in to the environment and timing the period until reception of a reflection[5, 34]. Low-power devices are used to measure distances typically not exceeding 50 metres. Accuracies are bounded by the stability of internal, very-high-frequency reference clocks required to time flight-paths at the speed of light[45]. More powerful lasers are susceptible to creating multipath reflections for proximate targets but have greater operating ranges. The firing rate may contribute to range errors: reflections from previously fired pulses alias in time with those from more recent pulses. Consequently laser ranging devices are only reliably operated only in environments where the maximum distance between any two points is known. Erroneous under-measurement of distances results when the firing rate is too high.

Devices might sample reflections from natural objects in the scene or with the assistance of optically-superior targets. Lunar laser ranging retroreflection (LLRR) offers extremely precise measurements— errors less than 0.001 m— of the distance between the moon and fixed, terrestrial base stations using three corner-cube retroreflectors left on the lunar surface by previous manned and unmanned visits[33]. In this case, corrections for the varying speeds of light in different media are necessary. Cloud cover contributes further corrections.

A common apparatus mounts a laser ranger on a motorised, steerable platform. As the platform orientation is adjusted the output dataset has uniform sample density in 3-dimensional steradian space, not in linear Cartesian space. The distinction is often neglected but distorted fish-eye images result.

---

[5]such antennae have Q between 10 and 25 and are commonly dimensioned to have 50 Ω impedance

Bibliography

[1] BAe innovations named millennium products. *Journal of Aerospace and Defense Industry News*, 6, November 1998.

> KEY: gyro:baesivsg
> ANNOTATION: Press coverage of BAe's VSG manufactured on the surface of a silicon integrated circuit. Three of the devices are used in each wing of Airbus aircraft.

[2] UK radio interface requirement 2030: Short range devices. Technical Report 2002/248/UK, Radio-communications Agency, Science and Technology Unit, Wyndham House, 189 Marsh Wall, London, E14 9SX, October 2002.

> KEY: rfid:ra
> ANNOTATION: The spectral power emission regulations for short range devices in the UK.

[3] Charles Broxmeyer. *Inertial Navigation Systems*, chapter 4. Electronic Sciences Series. McGraw-Hill Book Co., 1964.

> KEY: gyro:othertypes
> ANNOTATION: The fourth chapter includes descriptions of alternative gyroscopic devices: hermetic gyros, air floatation gyros, electrically suspended gyros (ESGs), and cryogenic gyros. The distinguishing features are highlighted and the continual strive to achieve support stiffness is compared. Vibrating structure gyros postdate this work.

[4] President William Jefferson Clinton. Statement by the president regarding the United States' decisions to stop degrading Global Position System accuracy (press release). *The White House Publications Office*, May 2000.

> KEY: gps:selectiveavailability
> ANNOTATION: President Clinton's official statement acting on his March 1996 pledge to improve the utility of GPS for civil and commercial activities by disabling selective availability with effect from midnight 2000-05-01. Military advantage is to be retained through demonstrated abilities to deny GPS on a regional basis.

[5] D.R. Crone. *Elementary Photogrammetry*. Edward Arnold Ltd, London, 1963.

> KEY: laserrange:elemphotogrammetry
> ANNOTATION: An introduction to the techniques of photogrammetry. The theory underlying hardware design construction is followed by the best practice of its operation.

[6] C.S. Draper, W Wrigley, and L.R. Grohe. The floating integrating gyro and its application to geometrical stabilisation problems on moving bases. *Aeronautical Engineering Review*, 15(6):42–62, June 1956.

> KEY: gyro:floated
>
> ANNOTATION: A seminal paper driven by Draper's long-standing research interests in gyroscopes. The paper presents the design and construction of a floated, integrating gyro, explaining carefully how contributing errors are eliminated or lessened by their design. The uses of the gyro device were then primarily aeronautical.

[7] Geoffrey Emmerson, David Victor Jolliffe, and Steven Paul Jolliffe. Identifying golf balls. Technical Report Patent number WO9948046, World Golf Systems Ltd., September 1999.

> KEY: rfid:golf
>
> ANNOTATION: Solves the problem of identifying your own golf ball without having to touch it. Unlike identifying surface paints, does not affect flight aerodynamics because RFID circuitry is internal.

[8] Manual Fernandez and George R Macomber. *Inertial guidance engineering*, chapter 3. Prentice-Hall space techology series. Prentice-Hall, 1962.

> KEY: gyro:inertialguidance
>
> ANNOTATION: A cronological tour of the evolution of gyroscope technology with a strong, scientific focus. Describes the different construction techniques, their distinctive advantages and disadvantages, and discusses the origin and magnitude of residual sources of error.

[9] Manual Fernandez and George R Macomber. *Inertial guidance engineering*, chapter 9. Prentice-Hall space techology series. Prentice-Hall, 1962.

> KEY: gyro:platformerrors
>
> ANNOTATION: Chapter 9 contains a mathematical treatment of the errors described in earlier in the work. The errors are quantised by expressions derived for their magnitudes in terms of the variables presented in the earlier chapters.

[10] Manual Fernandez and George R Macomber. *Inertial guidance engineering*, chapter 4. Prentice-Hall space techology series. Prentice-Hall, 1962.

> KEY: gyro:platform
>
> ANNOTATION: The fourth chapter of this work describes the construction and use of gyrostabilised platforms as a base for accelerometer triads. Builds on the third chapter to appreciate the gyroscopic errors and introduces the error in several pendulous and non-pendulous accelerometer designs. Finally, an overall statement of error is reached and practical techniques to lessen their effects are explained.

[11] A.P. French. *Vibrations and Waves*, pages 161–170. M.I.T. introductory physics series. Stanley Thornes, 1999.

KEY: vibstring:equations

ANNOTATION: Explains the physics behind vibrating string accelerometers, with equations. Movement of a central mass causes variations in the tensions of two anchoring strings, detected as variations in their natural (resonant) frequencies. The static friction holding the mass in place is a significant source of error.

[12] A.P. French and M.G. Ebison. *Introduction to Classical Mechanics*, pages 284–291. Chapman and Hall, 1997.

KEY: gyro:equations

ANNOTATION: A sound and clear presentation of the physics underlying gyroscopic phenomena. The discussion covers only rotating mass gyros but the equations apply equally to any angular momentum acted upon by a force in a field.

[13] Captain D. Glass. Notice to Mariners No.61/99 B14,C22,D12,E13,F26,G11: Withdrawal of General Lighthouse Authorities' Decca Navigator Service. British General Lighthouse Authority, Trinity House, London, EC3N 4DH, 21st December 1999.

KEY: radionav:deccaoff

ANNOTATION: Office Trinity House notice to mariners of the withdrawl of the Decca Navigator service. Three months notice was given by Captain D Glass.

[14] David House. *Navigation for Masters*. Witherby and Co. Ltd., London, 1995.

KEY: radionav:omega

ANNOTATION: Provides a consistent account of Decca, NavTex service, Marep service, channel navigation information service (CNIS, UK Dept. of Transport). Good source of information about the Omega worldwide LF radio navaid. 8 na.mi. accuracy. Used 8 1200 ft transmission towers, radiating 10 kW each at 10–14 kHz, gave independent fix every 10 s. Initial operating capacity in 1983; shutdown 0300Z Sept 30 1997. House also describes oceanic routing strategies robust to meteorological factors (storm prognosis, surface weather, sea temperatures, ice charts, etc.).

[15] Derek Howse. *Radar at Sea: the Royal Navy in World War II*. Macmillan, Basingstoke, 1993.

KEY: radionav:decca

ANNOTATION: Reviews the Gee (British Navy Outfit QH) and Decca (Outfit QM) navaids. Thorough description of the theory of operation of each. Decca: details implementation issues and use of L-series lattice charts. Howse also catalogues other World War II radio navaids and discusses their effectiveness. Excellent introduction; mathematical details not the focus.

[16] Robert Jenkins, John Leslie Duckett, and Ralph John Peter Dixon. Identification of livestock. Technical Report Patent number GB2289151, Private patent, November 1995.

KEY: rfid:cattle

ANNOTATION: Barcode tags for animal tracking in cattle auctions. Early, simple patent.

[17] Myron Kayton and Walter R. Fried, editors. *Avionics Navigation Systems*, chapter 9. John Wiley and Sons, Ltd., 1969.

KEY: celestial:electronic
ANNOTATION: Chapter 9 discusses celestial navigation, briefly covering the manual techniques used by early mariners before diving in to the details of modern, electronic celestial position fixing apparatus. Photovoltaic detectors, photoconductive detectors, and photoemissive devices are used to determine the relative positions of celestial bodies and position fixes computations are performed electronically using large reference tables.

[18] Myron Kayton and Walter R. Fried, editors. *Avionics Navigation Systems*, chapter 5. John Wiley and Sons, Ltd., 1969.

KEY: radionav:deccafreq
ANNOTATION: A thorough presentation of the alignment procedures for inertial navigation equipment, and the residual errors. The text covers the practice of achieving alignment in addition to the theory of the task.

[19] Alfred Leick. *GPS satellite surveying*. Wiley, New York; Chichester, second edition, 1995.

KEY: gps:survey
ANNOTATION: Describes the frequently-overlooked uses of GPS technology for surveying. Distinguishes precision and accuracy, and exploits the former quality of the Navstar GPS. Explores the mathematics of position fixing, relative position fixing, and time-dependent error characteristics in some detail. Includes anecdotes from field work.

[20] R Lownsborough and D Calcutt. *Electronic aids to navigation: radar and ARPA*. Edward Arnold, London, 1993.

KEY: radionav:radar
ANNOTATION: Describes RADAR and ARPA. Comprehensively covers RADAR: receiver circuits, propagation theory, errors, practical usage, theory of operation, explanation of choices of pulse lengths and frequencies, etc. ARPA (automatic radar plotting aid) is a modern-day automated RADAR unit.

[21] Ricard A Mabbott. Identification cards – contactless integrated circuit(s) cards – vicinity cards – part 1: Physical characteristics. Technical Report ISO/IEC 15693-1:2000, International Organization for Standardization, July 2000.

KEY: rfid:vicinity-phys
ANNOTATION: Describes the ISO15693 vicinity cards: similar in operation to proximity cards but in a different frequency band. See also [22, 23] and [25, 26, 27, 28].

[22] Ricard A Mabbott. Identification cards – contactless integrated circuit(s) cards – vicinity cards – part 2: Air interface and initialization. Technical Report ISO/IEC 15693-2:2000, International Organization for Standardization, May 2000. As corrected 2002-10-11, see [24].

KEY: rfid:vicinity-air
ANNOTATION: The radio protocol (data link) layer of the communications system for ISO
15693 cards, corrected in [24]. See [21].

[23] Ricard A Mabbott. Identification cards - contactless integrated circuit(s) cards - vicinity cards – part
3: Anticollision and transmission protocol. Technical Report ISO/IEC 15693-3:2001, International
Organization for Standardization, March 2001.

KEY: rfid:vicinity-pro
ANNOTATION: Describes the updated anti-collision protocol used by the ISO 15693 cards.
See [21].

[24] Ricard A Mabbott. Iso/iec 15693-2:2000/cor 1:2001. Technical Report ISO/IEC 15693-2:2000/Cor
1:2001, International Organization for Standardization, October 2001.

KEY: rfid:vicinity-air-cor
ANNOTATION: Technical corrections to [22]. See [21].

[25] Richard A Mabbott. Identification cards – contactless integrated circuit(s) cards – proximity cards –
part 1: Physical characteristics. Technical Report ISO/IEC 14443-1:2000, International Organization
for Standardization, April 2000.

KEY: rfid:identification-phys
ANNOTATION: Describes the tangible properties of ISO14443 cards: dimensions, mass,
surface textures, etc. and the physical radio components. See also [26, 27, 28] and [21, 22,
23].

[26] Richard A Mabbott. Identification cards – contactless integrated circuit(s) cards – proximity cards
– part 2: Radio frequency power and signal interface. Technical Report ISO/IEC 14443-2:2001,
International Organization for Standardization, June 2001.

KEY: rfid:identification-air
ANNOTATION: Describes the radio layer (ISO physical layer) of the communications stack
as applies to ISO14443 cards. See [25].

[27] Richard A Mabbott. Identification cards – contactless integrated circuit(s) cards – proximity cards
– part 3: Initialization and anticollision. Technical Report ISO/IEC 14443-3:2001, International
Organization for Standardization, February 2001.

KEY: rfid:identification-col
ANNOTATION: Describes the strategy adopted by the radio layer, and gives specific proto-
col details. Anticollision strategies are given particular attention due to their fundamental
rôle in RFID interrogation. See [25].

[28] Richard A Mabbott. Identification cards – contactless integrated circuit(s) cards – proximity cards –
part 4: Transmission protocol. Technical Report ISO/IEC 14443-4:2001, International Organization
for Standardization, January 2001.

KEY: rfid:identification-pro

ANNOTATION: Describes the protocol's provisions for arbitrary data transport. See [25].

[29] Pamela J Maki and Peter S Marshall. Accommodating bicycles at signalled intersections with loop detectors: a case study and example. *Compendium of Technical Papers for the 67th ITE Annual Meeting*, 1997.

KEY: makimarshall:loopshapes

ANNOTATION: The authors discuss the advantages of installing two, independent loop detectors per lane to separately detect bicycles and automotive traffic. This option is rare in practice due to the increased expense.

[30] Benjamin Maurin, Osama Masoud, and Nikolaos Papanikolopoulos. Monitoring crowded traffic scenes. In *The IEEE 5th International Conference on Intelligent Transportation Systems*, Singapore, September 2002.

KEY: its:crowds

ANNOTATION: The authors are striving to develop an illumination and shadow invariant image processing technique to detect people in crowded traffic scenes. Segmentation uses monocular visual light cameras. Optical flow is used instead of the more conventional background subtraction to avoid merging objects that move past one another. Each frame is handled individually and objects are represented as oriented bounding boxes. A one-to-one relationship between the objects in successive frames is assumed! The technique frequently detects adverts and posters as people but otherwise performs broadly as intended.

[31] William M Maynard. RFID tagging system for network assets. Technical Report Patent number US5949335, Sensormatic Electronics Corporation, September 1999.

KEY: rfid:net

ANNOTATION: Tracking assets in a switch room or server room by RFID tagging cables and devices. A handheld unit querying a database allows an operator to determine the purpose, history, and software/network services relating to each wire and device.

[32] Connie L. McClure. *Theory of Inertial Guidance*, chapter 1. Prentice-Hall International Inc., 34–36 Beech St, London, EC1, 1960.

KEY: inav:intro

ANNOTATION: A sound introduction to Inertial Navigation and the details of obtaining position given only second time-derivative telemetry (acceleration vectors). Includes "deduced reckoning," or "ded. reckoning," now ubiquitously corrupted to "dead reckoning."

[33] Charles W Misner, Kip S Thorne, and John Archibald Wheeler. *Gravitation*, chapter 40. W.H. Freeman and Company, New York, 1997.

KEY: laserrange:lunarlaserranging

ANNOTATION: Describes the technique of lunar laser ranging retroreflection using corner-cube reflectors left on the moon surface by previous manned and unmanned visits. A com-

prehensive discussion of errors is included, and many of the compensations that can be applied.

[34] Francis H Moffitt and Edward M Mikhail. *Photogrammetry*, chapter 11. Harper and Row (Publishers) Ltd, New York, third edition, 1980.

    KEY: laserrange:photogrammetry

    ANNOTATION: A comprehensive and mathematical treatment of photogrammetry.

[35] Dominick L Monico. Low cost long distance RFID reading. Technical Report Patent number US6259369, Patent by Moore North America Inc., July 2001.

    KEY: rfid:ink

    ANNOTATION: Electrically conductive, printable inks suitable for the construction of stable RFID antennae. The liquid base has appropriate viscosity to reliably print contacts with IC bond wires.

[36] W Oertel, T Dimter, and D Szoska. A video-based approach for stationary platform supervision. In *The IEEE 5th International Conference on Intelligent Transportation Systems*, Singapore, September 2002.

    KEY: its:platform

    ANNOTATION: Describes the KOMPAS project (Fraunhofer, Germany): goal is to stop people being hit by trains on platforms. Stereo video cameras are attached to the station and a 19" rack cabinet housing parallel video processing hardware performs soft real-time computation to send an "all-OK: safe" message every 100 ms unless a hazard is detected. Multiple cameras provide fault tolerance. Railway-specific knowledge is used to speed-up the image processing (e.g. train approach directions, appearance of rails and sleepers, etc.). Achieves VDV399 (German standard for object sizes that must be detected by railway safety systems). Installed at Dresden station and new subway in Berlin.

[37] Michail Order. Blackjack card game practice set-up. Technical Report Patent number US5941769, Private patent, August 1999.

    KEY: rfid:blackjack

    ANNOTATION: Electronic tagging of packs of 52 playing cards with the purpose of machine identification of dealt hands. Allows a card shuffling machine to interact with human players simultaneously with computerised opponents.

[38] George R. Pitman Jr., editor. *Inertial Guidance*, chapter 2. University of California Engineering and Physical Sciences Extension Series. John Wiley and Sons, Ltd., 1962.

    KEY: accel:intacc

    ANNOTATION: Discusses integrating accelerometers. The output is proportional to the time-integral of acceleration (velocity), or the double integral (position). Drift error accumulates with each integration and special precautions are necessary to prevent run-away error build-up.

[39] Richard H. Pravin. *Inertial Navigation*, chapter 6. Principles of Guided Missile Design. D. Van Nostrand Company, Inc., 120 Alexander St., Princeton, New York 18, New York, 1956.

    KEY: gyro:missile

    ANNOTATION: Discusses the mechanics and science of gyrostabilised platforms for the navigation and control of ballistic flights. Includes a discussion of alignment and other errors, and corresponding treatments.

[40] Richard H. Pravin. *Inertial Navigation*, chapter 8. Principles of Guided Missile Design. D. Van Nostrand Company, Inc., 120 Alexander St., Princeton, New York 18, New York, 1956.

    KEY: gyro:gimballock

    ANNOTATION: Chapter 8 describes gimbal lock, an effect whereby a 3 degree-of-freedom (3DF) gyro can be reduced to a 2DF device by unfortunate alignment of the gimbal frames. A fourth gimbal frame is required to resolve the problem and guarantee the ability of the gyro to respond to any movement in 3 dimensions. As is it necessary only when gimbal lock would otherwise ensue, the 4th is termed the "redundant" gimbal frame.

[41] Richard H. Pravin. *Inertial Navigation*, chapter 12–13. Principles of Guided Missile Design. D. Van Nostrand Company, Inc., 120 Alexander St., Princeton, New York 18, New York, 1956.

    KEY: gyro:errors

    ANNOTATION: Chapters 12 and 13 present qualitative and quantitative examinations of the errors present in inertial flight control systems. The discussion is detailed but limited in scope to the errors brought out by the application rather than general properties of the gyro and accelerometer devices.

[42] Howard S Seifert and Kenneth Brown. *Ballistic Missile and Space Vehicle Systems*, chapter 17, pages 402–447. University of California Engineering and Physical Sciences Extension Series. John Wiley and Sons, Ltd., 1961.

    KEY: gyro:courseinput

    ANNOTATION: Discusses the issues central to the inertial guidance of ballistic missiles. Relative location is derived from accelerations and gyrostabilised platforms are used. Course data are injected into the closed feedback loops of the gyro calibrations.

[43] Howard S Seifert and Kenneth Brown. *Ballistic Missile and Space Vehicle Systems*, chapter 16, pages 372–401. University of California Engineering and Physical Sciences Extension Series. John Wiley and Sons, Ltd., 1961.

    KEY: radionav:principles

    ANNOTATION: Explains the principles of radio navigation systems. A solid introduction to the topic.

[44] Ali Sheikholeslami and P Glenn Gulak. A survey of circuit innovations in ferroelectric random-access memories. *Proceedings of the IEEE*, 88(5):667–689, May 2000.

KEY: rfid:ferromemories

ANNOTATION: Describes the innovations since PROM, EERPOM, and Flash. Ferromagnetic memories were advanced to ferroelectric memories. The latter achieve low write-access times, and lower overall power consumption than EEPROM or Flash, making them particularly suitable for RFID.

[45] J.R. Smith. *Optical distance measurement*. Crosby Lockwood and Son Ltd, London, 1970.

KEY: laserrange:opticaldistance

ANNOTATION: A mathematical approach to distance measurement using optical hardware. Included is a discussion of the difficulties in precisely measuring the times-of-flight of signals travelling at the speed of light.

[46] John R Tuttle. Electrically powered postage stamp or mailing or shipping label operative with radio frequency (RF) communication. Technical Report Patent number US5497140, Micron Technologies Inc., March 1993.

KEY: rfid:postage

ANNOTATION: Construction of a postal sorting (and tracking) machines based on RFID-enabled postage stamps.

[47] United States Department of Defense. *Technical Characteristics of the NAVSTAR GPS (Navigation Satellite Timing and Ranging Global Positioning System)*, unclassified edition, June 1991.

KEY: gps:dodofficial

ANNOTATION: The official civilian documentation on the GPS constellation, orbital models, timing and ranging pseudorange algorithms, and operating bounds. Comprehensive discussion of the magnitude of user range errors, their physical origins, identifying features, and handling techniques. Since its publication the constellation has been extended with new orbital planes and additional carrier frequencies are now available to improve ionospheric modelling, but the geometry and algorithms remain relevant. A significant change was the removal of Selective Availability[4].

[48] Harini Veeraraghavan, Osama Masoud, and Nikolaos Papanikolopoulos. Vision-based monitoring of intersections. In *The IEEE 5th International Conference on Intelligent Transportation Systems*, Singapore, September 2002.

KEY: its:nearmiss

ANNOTATION: The authors want to detect collisions and near misses by image processing using blob-tracking. Adaptive background subtraction is performed initially but the subsequent tracking algorithm used is not robust to occlusions, shadows, or long stationary times. Each frame of video is handled independently and no ingress/egress points are used to assist the object tracker. Oriented bounding boxes are used to represent vehicles. Simple, rapidly executing method with acceptable results.

[49] Alan Watchel. Re-evaluating traffic signal detector loops. *Bicycle Forum*, (50):12–16, 2000.

KEY: watchtel:loopsforbikes

ANNOTATION: This follow-up article to Don Wood's original[52] discusses the shapes of induction loop detectors and compares their suitabilities for detecting bicycles at signalled intersections. In addition to studying the magnetic field patterns put out by, and the field-bicycle flux-linkage of alternative coil morphologies Watchel considers practical installation details, weather immunity, and mechanical endurance.

[50] W.S. Watson. Vibrating structure gyro performance improvements. Technical Report 19, Watson Industries, Inc, 3041 Melby Road, Eau Claire, Wisconsin, USA 54703, September 2000.

KEY: gyro:watson

ANNOTATION: Describes a collection of design improvements to the basic VSG design. Carefully shaped drive and sense electrodes reduce distortion. Manufacturing techniques to increase machining tolerances are described. A keyed cup shape is suggested to reduce harmonic effects and internal cabling arrangements used to prevent mechanical interference with the vibratory motion.

[51] Roy Williams. *Geometry of Navigation*. Ellis Horwood series in mathematics and its applications. Horwood Publishing, Chichester, 1998.

KEY: celestial:sphgeom

ANNOTATION: Presents the mathematics of celestial spherical geometry. Includes details of transformations routines to convert co-ordinates between celestial reference frames. Also includes projection algorithms: mapping celestial frames of reference onto local flat-earth models.

[52] Don Wood. Evaluating traffic signal detector loops. *Bicycle Forum*, (45):4–5, June 1997.

KEY: wood:loopsforbikes

ANNOTATION: Wood describes the problems facing cyclists in California due to the induction loop detectors at signalled intersections failing to reliable detect the presence of cyclists. He compares the magnetic field patterns of the prominent morphologies seen on California's highways.